Shock Melting of a Two-Dimensional Complex (Dusty) Plasma

D. Samsonov,[1] S. K. Zhdanov,[1] R. A. Quinn,[1] S. I. Popel,[2] and G. E. Morfill[1]
[1]*CIPS, Max-Planck-Institut für Extraterrestrische Physik, D-85740 Garching, Germany*
[2]*Institute for Dynamics of Geospheres RAS, Leninsky prospect 38/1 119334 Moscow, Russia*
(Received 28 October 2003; published 23 June 2004)

Shock waves with a linear front were experimentally studied in a monolayer hexagonal Yukawa lattice which was formed from charged monodisperse plastic microspheres and levitated in the sheath of a radio-frequency discharge. It was found that the shock can cause phase transitions from a crystalline to gaslike and liquidlike states. Melting occurred in two stages. First, the lattice was compressed in the direction of shock propagation and second, the particle velocities were randomized a few lattice lines downstream. The Mach number of the shock reached 2.7.

DOI: 10.1103/PhysRevLett.92.255004 PACS numbers: 52.27.Lw, 47.40.Nm, 52.35.Tc, 62.50.+p

A shock wave is usually described as a propagating disturbance characterized by an extremely rapid rise in pressure, temperature, and density [1]. It cannot be treated as a linear small-amplitude wave; instead the usual treatment is that of a discontinuity with a width of a few mean free paths. Shocks have been studied in gases, solids, plasmas, and granular media.

In gas dynamics, the "strength" of the shock waves is quantified by the pressure ratio in front and behind the shock. If it is close to unity, the shock is weak. If it is much larger than unity, the shock is strong.

In solids, shocks are categorized by the damage they inflict. An elastic shock is characterized by nondamaging stresses below the elastic limit. An elastic-plastic shock causes plastic deformations. Strong shocks melt or even vaporize the solid. Thus, shocks can produce phase transitions.

Complex (dusty) plasmas can spontaneously form ordered (crystalline) structures [2,3], so-called "plasma crystals." Plasma crystals are unique because they have weak damping compared to colloids [4] and the lattice waves are not overdamped. The characteristic eigenmode frequencies are low (<100 Hz) compared to ordinary crystals and hence even rapid processes can be visualized at the kinetic level comparatively easily. These properties make plasma crystals good model systems for studying nonlinear dynamical processes such as the solid-liquid phase transitions.

There are other systems (apart from natural crystals) which can be used to study phase transitions. Examples from low-temperature physics and quantum optics are the so-called "Wigner" crystals [5], ion and electron crystals. Because of their small size and high eigenmode frequencies these systems are very difficult to study.

It was shown in previous work that weakly coupled complex plasmas (gaseous phase) can sustain dust ion acoustic (DIA) and dust acoustic (DA) shock waves. DIA shocks were studied experimentally in [6] and theoretically in [7]. DA shocks were observed in a microgravity experiment onboard the International Space Station [8], they were described theoretically [9], and modeled by a molecular dynamics (MD) simulation [10]. In strongly coupled complex plasmas (crystalline phase) Mach cone shocks were reported [11,12], these shocks were weak and did not induce a phase transition.

Here we report an experimental observation (at a kinetic level) of a shock wave of sufficient strength to melt the plasma crystal, through which it propagates.

The experiments were performed in a setup (Fig. 1) similar to that of Ref. [13] using a capacitively coupled radio-frequency (rf) discharge. The discharge chamber had a lower disk electrode and an upper ring electrode. The upper electrode and the chamber were grounded. A rf power of 10 W (measured as forward minus reverse) was applied to the lower electrode. An argon gas flow at a rate of 0.5 sccm maintained the working gas pressure of 1.8 Pa in the chamber. Monodisperse plastic microspheres 8.9 ± 0.1 μm in diameter were levitated in the sheath above the

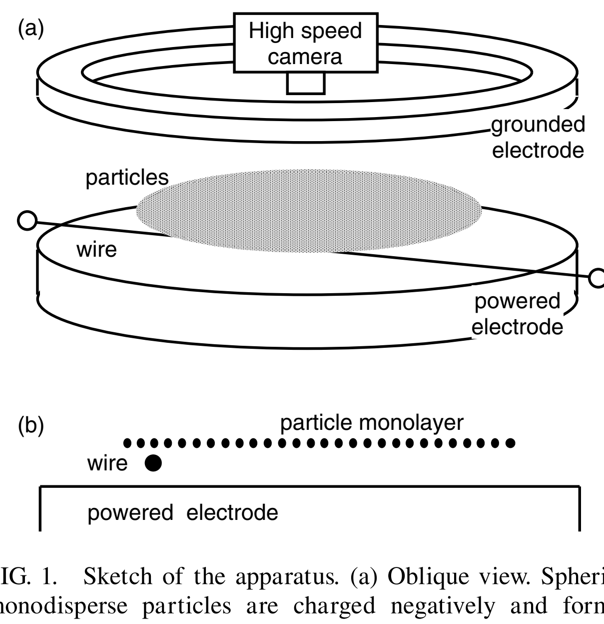

FIG. 1. Sketch of the apparatus. (a) Oblique view. Spherical monodisperse particles are charged negatively and form a monolayer, levitating in the plasma sheath above the lower electrode. (b) Side view. Short negative pulses applied to the wire (placed below the lattice) excite shocks.

 0031-9007/04/92(25)/255004(4)$22.50

lower electrode forming a monolayer hexagonal lattice. They were confined radially in a bowl shaped potential formed by a rim on the outer edge of the electrode. The monolayer particle cloud was about 6 cm in diameter and levitated at a height of $\simeq$9 mm above the lower electrode. The particle separation in the lattice was 650 μm at the excitation edge (Fig. 1), 550 μm in the middle, and 720 μm at the outer edge. The particles were illuminated by a horizontal thin (0.2–0.3 mm) sheet of light from a doubled Nd:YAG (Nd-doped yttrium aluminum garnet) diode pumped laser (532 nm) and imaged by a top view digital video camera at 102.56 frames/s. The field of view was 1024×512 pixels or 4.42×2.21 cm and it contained about 3000 particles.

A horizontal tungsten wire 0.1 mm in diameter was placed 4 mm below the particle layer and roughly half way between the center and the edge of the electrode. The wire was normally grounded so that it had little influence on the particles. A short negative pulse (-100 V, 50 ms) applied to the wire 0.07 s after the start of recording pushed the particles away, breaking the lattice above the wire and creating a pulsed compressional disturbance with a sharp linear front, which propagated horizontally in the direction perpendicular to the wire. The crystal was shock melted behind the front. The excitation pulse was much stronger than in the previous experiment (-30 V, 100 ms, [13]) where solitons were excited. As the pulse propagated (see a movie at [14]) and weakened it was seen that the shock-melting ceased, roughly in middle of the field of view (Fig. 2). The lattice also oscillated in the vertical direction with a small amplitude which caused a periodic change of particle brightness. A time interval of about 1 min was sufficient for the lattice to come into equilibrium and recrystallize.

For the quantitative analysis of our experiment, we identified the particle positions in the sequences of video images. Tracing of the particle motion in consecutive frames yielded their velocity, which was then averaged in 50 narrow bins parallel to the wire. The average velocity corresponded to the flow induced by the shock. The kinetic temperature was calculated from the standard deviation of the particle velocity in the bins which depends only on the particle random motion (both parallel and perpendicular to the front). We used a Voronoi analysis (a standard technique) to determine the local number density and the number of nearest neighbors. The *compression factor* was defined as the ratio of the actual particle number density to the unperturbed value. The *defect fraction* was defined as the fraction of non–six-fold Voronoi cells. All measured quantities were binned to reduce the influence of random fluctuations.

To visualize the pulsed perturbation we plotted grayscale maps of the *compression factor* [Fig. 3(a)] and *kinetic temperature* [Fig. 3(b)]. A narrow compression peak [Fig. 3(a)] propagated at a speed of 55 mm/s to the middle of the field of view, slowing down to 28 mm/s at the end. Using small compression ripples (see Fig. 2 in Ref. [13]) we can measure the dust-lattice wave speed

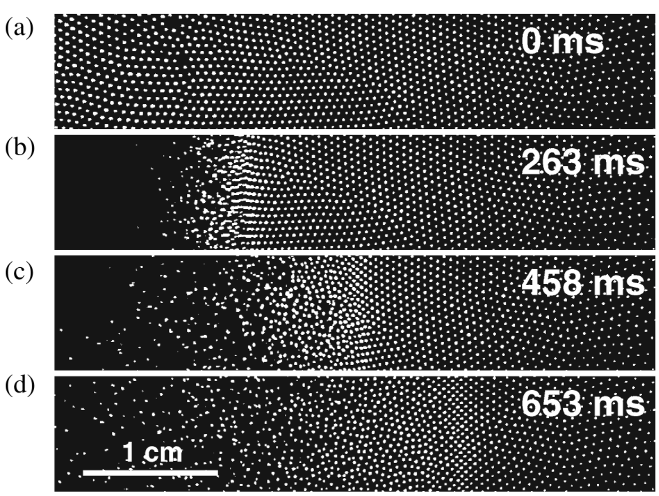

FIG. 2. Shock wave propagating in a monolayer hexagonal lattice. The excitation pulse was applied to the wire placed at the left edge of the field of view 2 mm below the lattice plane. Initially undisturbed particles (at 0 ms) were swept from left to right (at 263 and 458 ms) forming a shock with a sharp linear front. The lattice melted behind the front. At later times (653 ms) the amplitude of the disturbance reduced due to the neutral drag and a soliton was formed.

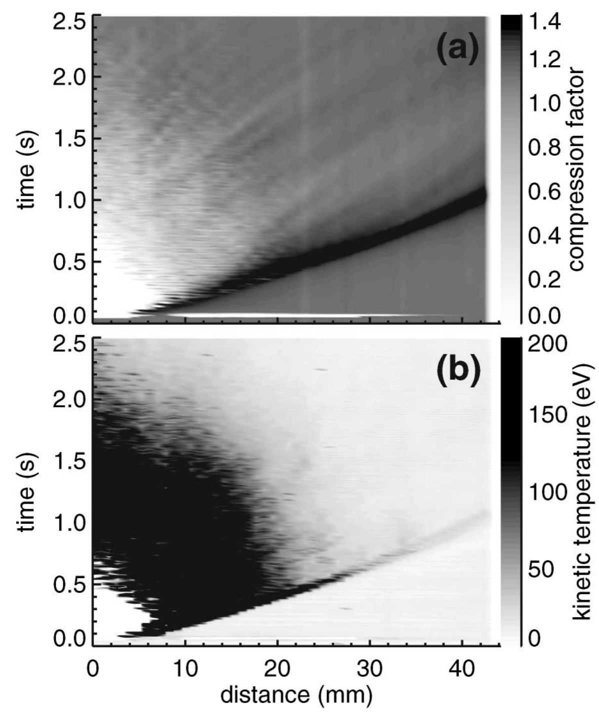

FIG. 3. Visualization of the experimentally observed shock with Mach number 2.7. (a) compression factor, (b) particle kinetic temperature as a function of time and distance to the wire. The shock is characterized by a narrow compression peak propagating at supersonic velocity. The kinetic temperature has a jump at the shock front. The crystal is melted behind the shock. It recrystallizes after about 5 s.

C_{DL} in the middle of the lattice. It was 23 mm/s (note that the plasma and the lattice conditions were identical here and in Ref. [13]). Taking the observed particle number density changes into account we calculated the Mach number of the perturbation $M = 2.7$ at the excitation region, $M = 2.4$ in the middle, and $M = 1.5$ at the end of the field of view.

The structure of the propagating disturbance is shown in Fig. 4 at 0.38 s when the front is roughly in the middle of the field of view. The *compression factor* [Fig. 4(a)] is unity in the unperturbed region; it rises to about 1.2 at the front and then decreases due to the relaxation of the dust cloud in the downstream excitation region. Note that the excitation pulse is very short and does not prevent the backflow of the particles to their equilibrium position behind the perturbation front. The 2D particle *number density* [Fig. 4(b)] changes from its unperturbed value of 4.0 mm^{-2} to 4.8 mm^{-2} after the pulse passes. The particle *directed flow speed* [Fig. 4(c)] is zero before the pulse, it peaks at the front, and drops to negative values due to the backflow. The *defect fraction* [Fig. 4(d)] is low before the disturbance (the plasma is highly ordered), and it increases behind the front indicating destruction of the crystalline structure. The particle *kinetic temperature* [Fig. 4(e)] is about 0.5 eV in the unperturbed lattice, it rises to about 300 eV behind the perturbation.

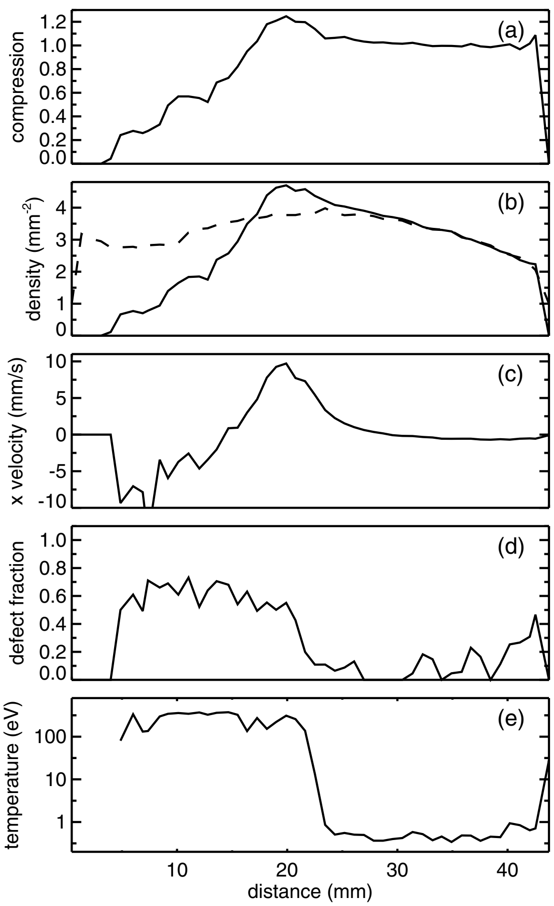

FIG. 4. Structure of the experimentally observed shock front at time 0.38 s. (a) compression factor, (b) particle number density (dashed line indicates unperturbed number density), (c) particle velocity in the direction of the shock propagation, (d) defect fraction, and (e) particle kinetic temperature, plotted versus distance to the excitation source. The compression factor, number density, and particle speed have a peak at the shock front, whereas the defect fraction and the kinetic temperature have a jump.

The observed supersonic perturbation can be identified as a shock because the particle kinetic temperature [Fig. 4(e)] and the defect fraction [Fig. 4(d)] have a jump, and there is particle transfer through the front, which propagates into a stationary medium. The particle flux j is described by the first Hugoniot relation [1] written for a linear shock in a 2D geometry [12]

$$j \equiv n_2(V - v_2) = n_1 V, \tag{1}$$

where V is the shock propagation velocity, v_2 is the component of the particle velocity normal to the shock front, n is the two-dimensional particle number density, and the indices 1 and 2 denote the condition ahead and behind the shock, respectively. In the laboratory frame $v_1 = 0$. For the experimental parameters determined from Fig. 4, $V = 55$ mm/s, $v_2 = 10$ mm/s, $n_1 = 4.0\ \mathrm{mm}^{-2}$, $n_2 = 4.8\ \mathrm{mm}^{-2}$, we find that the left- and right-hand sides of Eq. (1) match within a few percent, comparable with our measurement errors. The flux $j = 220\ \mathrm{mm}^{-1}\,\mathrm{s}^{-1}$.

The observed shock causes melting of the plasma crystal. Shock melting is expected to be very different from the melting transition already studied in [15] under near equilibrium conditions. Figure 2 reveals the kinetics of the shock melting. It appears [Figs. 2(b) and 2(c)] that the crystal is first compressed at the shock front without breaking the lattice structure at this time. The particles move only in the direction of the shock propagation. The melting and randomization of particle motion occurs about 5–7 lattice lines behind the compressed region. This differs significantly from the homogeneous melting experiment [15], where the kinetic temperature was increased slowly everywhere as contrasted to our almost instantaneous localized heating.

The kinetic temperature changes from about 0.5 eV before the shock to about 300 eV after the shock (at time 0.38 s). This corresponds to change in the coupling parameter Γ from $\sim$1300 to $\sim$2, calculated using the value of the particle charge $Q = 16\,000e$ estimated from the dust-lattice wave speed. Γ is defined as the ratio of the particles' potential (Coulomb) energy to their kinetic energy. From theory [16] and molecular dynamics simulation [17] the phase transition is expected to occur at $\Gamma \gtrsim 200$.

As the shock propagates its strength changes. At early times it even appears that it may have caused a sublimation transition with particles moving very fast in and out of the laser sheet and no structure discernible. Later, after

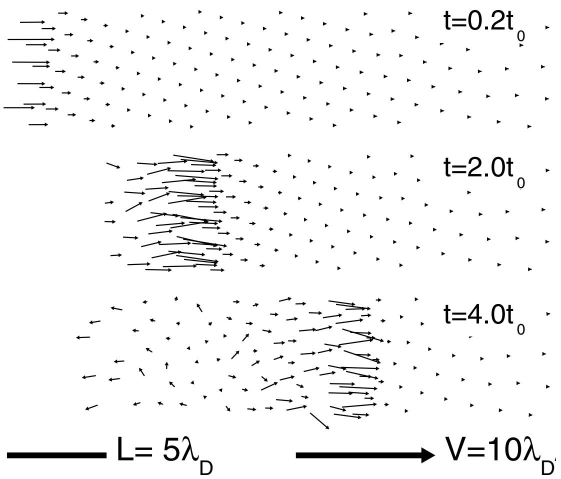

FIG. 5. Velocity vector map of a three-dimensional molecular dynamics simulation (MDS) of a shock in a monolayer hexagonal lattice. The shock propagates melting the lattice. The length scale L, velocity scale V, and time t are expressed in terms of Debye length λ_D and time scale $t_0 = \sqrt{m\lambda_D^3/Q^2}$, where m and Q are the particle mass and charge, respectively.

0.3–0.7 s the shock melts the crystal. The grains remain in the illuminated plane and it is possible to trace their motion. The particle separation remains approximately constant, while the orientational structure disappears. At later times when the shock becomes weak, it does not melt the crystal and turns into a dissipative soliton (see also [13]).

Nonlinear compressional pulses (identified as dissipative solitons) were observed before in the experiments using wire excitation [13] with the compression factor n_2/n_1 reaching 1.15 and the Mach number 2.1. Another experiment [18] produced pulses using laser excitation with n_2/n_1 up to 1.1 and the Mach number 1.3. Neither pulse steepening nor plastic deformations were reported in Refs. [13,18]. A slightly higher $n_2/n_1 = 1.2$ obtained here is responsible for a phase transition. It is well known [1] that while the pressure can infinitely increase behind the shock (for strong shocks), e.g., for an ideal gas n_2/n_1 is limited by the value $(\gamma + 1)/(\gamma - 1)$, $\gamma = c_p/c_v$, where c_p, c_v are the heat capacities at constant pressure and volume. Thus a slightly higher compression can result in a significant pressure increase.

A molecular dynamics simulation (MDS) was performed in order to understand and interpret the experimental results. We used a monolayer lattice formed of 721 particles in a three-dimensional confining potential. The lattice was strongly confined in the vertical direction and weakly in the horizontal plane. Simulation parameters were chosen from the experiment. The particles interacted via a screened Coulomb (Yukawa) potential and their motion was damped by neutral gas friction. They were initially placed at random positions and allowed to equilibrate by running the code until a stable hexagonal lattice was formed. The crystal was then excited by a pulsed force field which was approximated by a function which decayed exponentially with distance from the wire. The amplitude was chosen so that it produced the same particle speeds as in the experiment. The force was applied for the time equal to that of the experiment and then switched off.

Figure 5 shows a part of the simulated lattice with the propagating shock wave. MDS reproduces the features of the shock observed in the experiment, such as the linear well-defined shock front, compression at the front without melting, velocity randomization and melting a few lattice lines downstream, reduction of the shock amplitude in time as it propagates. We did not observe decay of the shock into a soliton since the lattice had significantly fewer particles than in the experiment. The shock had too short a distance to propagate. Also the simulated lattice had a stronger number density gradient which caused a "tsunami effect" or steepening of the wave front in the right part of the crystal and thus interfered with soliton formation. However, we were able to produce solitons using weak excitation pulses. MDS did not take into account the motion of individual ions and electrons which we believe influence the grains only though the interaction and confining potentials.

S. I. P. was supported by INTAS (Grant No. 01–0391) and RFBR (Grant No. 03-02-16664-a).

[1] J. Bond, K. Watson, and J. Welch, *Atomic Theory of Gas Dynamics* (Addison-Wesley, Massachusets, 1965).
[2] J. Chu and I. Lin, Phys. Rev. Lett. **72**, 4009 (1994).
[3] H. Thomas *et al.*, Phys. Rev. Lett. **73**, 652 (1994).
[4] M. Hoppenbrouwers and W. van de Water, Phys. Rev. Lett. **80**, 3871 (1998).
[5] E. Wigner, Phys. Rev. **46**, 1002 (1934).
[6] Y. Nakamura, H. Bailung, and P. K. Shukla, Phys. Rev. Lett. **83**, 1602 (1999).
[7] S. I. Popel, M. Y. Yu, and V. N. Tsytovich, Phys. Plasmas **3**, 4313 (1996); S. I. Popel, A. P. Golub', and T. V. Losseva, JETP Lett. **74**, 362 (2001).
[8] D. Samsonov *et al.*, Phys. Rev. E **67**, 036404 (2003).
[9] F. Li and O. Havnes, Phys. Rev. E **64**, 066407 (2001).
[10] J. E. Hammerberg, T. C. Germann, and B. L. Holian, in AIP Conf. Proc. No. 1 (AIP, New York, 2002), pp. 359–362.
[11] D. Samsonov *et al.*, Phys. Rev. Lett. **83**, 3649 (1999).
[12] D. Samsonov *et al.*, Phys. Rev. E **61**, 5557 (2000).
[13] D. Samsonov *et al.*, Phys. Rev. Lett. **88**, 095004 (2002).
[14] D. Samsonov *et al.*, movie of a shock in a two-dimensional complex (dusty) plasma, http://www.mpe.mpg.de/~dms/movies/index.html
[15] H. Thomas and G. Morfill, Nature (London) **379**, 806 (1996).
[16] H. Ikezi, Phys. Fluids **29**, 1764 (1986).
[17] R. Farouki and S. Hamaguchi, Appl. Phys. Lett. **61**, 2973 (1992).
[18] V. Nosenko, S. Nunomura, and J. Goree, Phys. Rev. Lett. **88**, 215002 (2002).